

## The Platinum-Catalyzed Oxidation of 2-Propanol

ROBERT L. AUGUSTINE AND LISA K. DOYLE

*Department of Chemistry, Seton Hall University, South Orange, New Jersey 07079*

Received June 29, 1992; revised November 3, 1992

The platinum-catalyzed oxidation of 2-propanol was run over a series of single-turnover (STO) characterized Pt/CPG (Controlled Pore Glass) catalysts. Comparison of reaction rates with STO site densities showed that the oxidation was taking place on the more coordinatively unsaturated corner atoms on the catalysts. Specific site TOFs were found to be 5.5, 7.9, and 5.0 moles O<sub>2</sub> uptake/mole of site/min for the <sup>3</sup>M<sub>I</sub>, <sup>3</sup>M<sub>R</sub>, and <sup>3</sup>MH sites, respectively. Initial rate data were obtained for reactions run at several 2-propanol concentrations at three separate oxygen pressures. These data were analyzed using the double reciprocal Lineweaver–Burke method commonly employed in enzyme kinetic determinations. The data obtained showed that oxygen was adsorbed about 200 times more strongly than 2-propanol in these reactions. A maximum rate value of 18 moles of O<sub>2</sub> consumed/mole of active site/min was calculated. This value represents the maximum rate for the reaction when it is run under zero-order conditions for both reactants without diffusion limitations. The present data were obtained, however, under first order reaction conditions. Given the difference in reaction conditions, the experimentally determined TOF of 6 min<sup>-1</sup> is not an unreasonable value. © 1993 Academic Press, Inc.

### INTRODUCTION

The noble-metal-catalyzed oxidation of alcohols has potential synthetic utility but, at present, its use appears to be limited to the oxidations of water-soluble substrates. Over the years there have been a number of reports published about this reaction (1–33). Primary alcohols are oxidized to acids in basic media but, to a lesser extent, to aldehydes in neutral or acidic solutions. Secondary alcohols are oxidized to ketones with no apparent over oxidation (1). An aqueous medium is most commonly used but there are a few reports of the use of organic solvents (3–6). This reaction is very selective, oxidizing primary hydroxy groups in the presence of secondary alcohols and axial alcohols in preference to equatorial hydroxy groups (1, 6–10). Platinum is the most common catalyst with palladium used less frequently (1, 11, 12). The oxidation takes place under ambient conditions usually at slightly elevated oxygen pressures. One problem is the catalyst deactivation arising

from the oxidation of the metal catalyst. The order of resistance to this deactivation was found to be Pt > Ir > Pd > Rh > Ru (12). Running the reaction under partial pressures of oxygen minimizes metal oxidation but also slows down the alcohol oxidation (11).

Reported mechanistic data support the hypothesis that this reaction proceeds by way of an initial dehydrogenation followed by the oxidation of the hydrogen by oxygen (11, 28–33). The rate-determining step appears to be the cleavage of the C–H bond on the carbinol carbon (11, 30, 33).

With all of the reports on this reaction there are still a number of questions still needing answers. In the first place the type of surface site on which this reaction is taking place needs to be identified. The C–H bond breaking in the aromatization of cyclohexane has been shown to occur on corner or kink atoms on the catalyst (34, 35) so, by analogy, it would be expected that the C–H bond cleavage in alcohol dehydrogenation should also take place on corner atoms. However, in the oxidation of 2-propanol,

catalysts with low dispersions had higher initial activities than those with high dispersions (11). This indicates that the oxidation may be taking place on the faces of the larger metal crystallites present in low dispersion catalysts.

Secondly, while some kinetic studies of this reaction have been reported, much of the data were acquired under diffusion control conditions so no mechanistic conclusions could be drawn (11). A more complete kinetic examination of this reaction is needed. Finally, there is the matter of the commonly used aqueous reaction medium and the reason for the catalyst deactivation usually encountered. It must be determined whether water is needed for this reaction and, if so, why. The catalyst deactivation should also be investigated to see if it is brought about, at least in part, by a competitive adsorption between product, reagent and solvent.

The present manuscript is concerned with the first two of these while the others will be the subject of a future publication.

#### EXPERIMENTAL

The 3.35% Pt/CPG (Controlled Pore Glass) catalysts and the 8% Pt/SiO<sub>2</sub> catalyst were prepared by ion exchange using an aqueous solution of H<sub>2</sub>PtCl<sub>6</sub> and following the procedure described previously (36). Samples of the 3.35% Pt/CPG catalyst precursor salt were reduced isothermally under H<sub>2</sub> at 200, 250, 300, and 400°C, and under H<sub>2</sub> with the temperature ramped from 50 to 400°C at 40°C/min following the procedures described in the literature (37). The 8% Pt/SiO<sub>2</sub> precursor salt was reduced under H<sub>2</sub> with the temperature ramped from 50 to 200°C at 10°C/min. Analysis of the reduced species showed that all of the chlorine had been removed during the reduction procedure. All water used in this study was doubly distilled.

#### *Chemisorption Measurements*

All chemisorption studies were carried out using an Omnisorp 100CX apparatus.

Samples (about 0.5–1.0 g) were placed in a Pyrex cell and heated at a rate of 20°C/min to 100°C then He was passed through the sample for 10 min at a rate of 20 cc/min. The temperature was further increased to 150°C and the sample was exposed to a flow of hydrogen for 30 min. Following this step, the samples were evacuated to 10<sup>-5</sup>–10<sup>-6</sup> kPa with a simultaneous increase of the temperature to 300°C. At that point the evacuation was continued for 2 h followed by cooling to 40°C under vacuum. Successive calibrated pulses of H<sub>2</sub> were admitted into the sample and the pressure was monitored after each pulse until it reached equilibrium which usually was about 10–15 min after the admission of the pulse. A total of 20–25 pulses was commonly used to reach a pressure of 30 kPa. Following the first chemisorption, the samples were evacuated for 30 min at pressures of about 10<sup>-4</sup>–10<sup>-5</sup> kPa at the same temperature and the second chemisorption was measured. From these two sets of data, the first isotherm gave the values for both strongly and weakly adsorbed H<sub>2</sub> whereas the second isotherm represents the quantity of the "weakly or reversibly" adsorbed species.

#### *Single-Turnover Measurements (STO)*

The STO apparatus, reaction sequence and pulse injection techniques have already been described (38). A 5-mg sample of each catalyst was placed in the STO reactor (6-mm Pyrex tube). The reactor was purged with oxygen-free He for 30 min and the STO characterization sequence initiated. As usual, several initial STO sequences were required to remove the surface oxygen from the catalyst and to obtain reproducible results from further sequential STO reactions. The sequences consisted of an initial 20 μl pulse of H<sub>2</sub> to saturate the metal surface, followed after 2 min by a same pulse size of 1-butene to react with the adsorbed H<sub>2</sub>, producing butane from the direct, <sup>3</sup>M, hydrogenation sites and *cis*- and *trans*-2-butene from the <sup>2</sup>M isomerization sites. A second H<sub>2</sub> pulse, performed 6 min after the

TABLE 1

STO Site Densities<sup>a</sup> and Chemisorption Data for the Pt/CPG and Pt/SiO<sub>2</sub> Catalysts Used in the 2-Propanol Oxidations

Catalyst	Red'n temp. <sup>b</sup>	<sup>3</sup> M <sub>I</sub>	<sup>3</sup> M <sub>R</sub>	<sup>3</sup> MH	<sup>2</sup> M	<sup>1</sup> M	H <sub>Adsorbed</sub> <sup>c</sup>	% Dispers. <sup>d</sup>
3.35% Pt/CPG	200°C	0.220	0.058	0.105	0.078	0.176	0.895	62.7
3.35% Pt/CPG	250°C	0.201	0.046	0.086	0.088	0.181	0.849	60.2
3.35% Pt/CPG	300°C	0.204	0.050	0.111	0.081	0.219	0.919	66.5
3.35% Pt/CPG	400°C	0.295	0.053	0.140	0.076	0.000	0.901	56.4
3.35% Pt/CPG	50°–400°C 40°C/min	0.310	0.058	0.132	0.112	0.008	0.988	62.0
8.0% Pt/SiO <sub>2</sub>	50°–200°C 10°C/min	0.031	0.021	0.021	0.040			

<sup>a</sup> Site densities in (mole site)/(moles Pt total). Experimental error in determining site densities is  $\pm 5\%$ .

<sup>b</sup> Hydrogen reduction temperatures of Pt/CPG catalysts.

<sup>c</sup> Catalyst dispersion based on a 1 : 1 H : Pt atom stoichiometry.

<sup>d</sup> Dispersion values as (moles Pt surface sites)/(moles Pt total)  $\times 100$ .

1-butene pulse, was passed over the catalyst to react with the stable half-hydrogenated metalalkyl species still present on the metal surface, releasing the "second" butane in an amount equal to the number of the <sup>3</sup>MH, two-step, hydrogenation sites. Increasing the time between the first hydrogen and the 1-butene pulse to 60 min provides the numbers for <sup>3</sup>M<sub>I</sub> and <sup>3</sup>M<sub>R</sub> site densities. All products were analyzed by on-stream gas chromatography. Catalyst characterization data are found in Table 1 with site density data determined with an experimental error of  $\pm 5\%$  (38).

### Kinetic Studies

The 2-propanol oxidation rates that were used in the STO rate analysis and listed in Table 2 were determined by monitoring the oxygen uptake using a sloping manifold apparatus (39). For a typical reaction, 2 ml of 2-propanol in 15 ml of water were oxidized over 50 mg of 3.35% Pt/CPG at 20°C under one atmosphere of oxygen. The reaction flask was jacketed with thermostatted water circulated through the jacket to maintain a constant reaction temperature. The reaction solutions were agitated using a shaker. To verify that the reaction was being run in the

kinetic regime, the reaction rate was also determined for each of the catalysts using about 20–30% less catalyst. In all cases the rate per unit quantity of catalyst remained the same within an experimental error of  $\pm 5\%$  so the reactions were not mass transport limited. At the conclusion of the run the catalyst was removed by filtration. GC analysis of the reaction mixture showed that acetone was the only oxidation product formed.

The oxidation rate data used in the Ping-Pong kinetic analyses were also obtained by monitoring oxygen uptake but a computer controlled automated gas uptake apparatus

TABLE 2

Observed and Calculated TOF Values (moles O<sub>2</sub>/mole Pt/min) for 2-Propanol Oxidations Run over a Series of Pt/CPG Catalysts

Catalyst	Observed TOF	Calculated TOF
200°C	2.02 ( $\pm .10$ )	1.96 ( $\pm .10$ )
250°C	1.57 ( $\pm .08$ )	1.75 ( $\pm .09$ )
300°C	1.81 ( $\pm .09$ )	1.91 ( $\pm .10$ )
400°C	2.50 ( $\pm .13$ )	2.51 ( $\pm .13$ )
50°–400°/40°C	2.69 ( $\pm .14$ )	2.54 ( $\pm .13$ )

TABLE 3

Rates of 2-Propanol Oxidation Using a Pt/SiO<sub>2</sub> Catalyst at Various Partial Pressures of O<sub>2</sub>

[2-propanol]	Rate (moles oxygen consumed/minute/mole Pt)		
	760 mm oxygen	300 mm oxygen	235 mm oxygen
0.0 M	0.0	0.0	0.0
0.044 M	—	—	0.49 (±.02)
0.058 M	0.78 (±.04)	0.70 (±.03)	—
0.066 M	0.94 (±.05)	0.82 (±.04)	0.64 (±.03)
0.075 M	—	—	0.76 (±.04)
0.088 M	1.23 (±.06)	1.03 (±.05)	0.72 (±.04)
0.11 M	—	1.07 (±.05)	0.84 (±.04)
0.13 M	1.45 (±.07)	1.21 (±.06)	—
0.18 M	1.77 (±.09)	—	—

(40) was used. Aqueous 2-propanol solutions (15 ml) of varying molarities were oxidized at 20°C using 10-mg portions of the 8% (Pt/SiO<sub>2</sub>) catalyst under one atm of oxygen as well as under 300 and 235 Torr partial pressure of oxygen. The results are listed in Table 3. All runs were conducted under one atm total pressure with He added to those reactions using less than an atmosphere of O<sub>2</sub>. The reaction vessel was jacketed with thermostatted water and agitated using a shaker. The catalyst quantity was decreased by 50% in duplicate runs at each oxygen pressure. The rate per unit of catalyst remained within the experimental error of ±5% showing that the experimental data were not being obtained under mass transport conditions.

#### RESULTS AND DISCUSSION

Even though the surface of metal catalysts are generally considered to be composed of different types of sites having varying adsorption and reaction characteristics, the catalyst surface is usually assumed to be uniform to simplify the analysis of experimental data. This can present a problem in interpreting rate data, for instance, when the catalyst surface is composed primarily of unreactive sites with only a small number of the surface sites promoting a specific reaction. In such cases the areal TOF would

not provide any indication of the true activity of the active sites. In such a situation the comparison of rate data obtained from different catalysts would be rather tenuous. In order to obtain specific site rate data, it is first necessary to determine the number of different kinds of active sites present on a specific catalyst and then evaluate the activity of each toward the desired reaction.

#### Identification of the Nature of the Active Sites

The single turnover (STO) reaction sequence has been used to measure the amounts of five different types of surface sites present on a variety of dispersed metal catalysts (38, 41). There are two types of sites which promote the direct saturation of an alkene, one has strongly adsorbed hydrogen and the other has the hydrogen more weakly held. These have been termed <sup>3</sup>M<sub>1</sub> and <sup>3</sup>M<sub>R</sub>, respectively. There are also two-step saturation sites, <sup>3</sup>MH, isomerization sites, <sup>2</sup>M, and sites which adsorb hydrogen but do not take part in a double-bond hydrogenation, <sup>1</sup>M. It has been shown that all of the <sup>3</sup>M sites are the more coordinately unsaturated corner atoms or adatoms on the metal particles (35). It is presumed from other considerations (42–45) that the <sup>2</sup>M sites are edge atoms and <sup>1</sup>M sites are on the faces of the crystallites (35). To determine

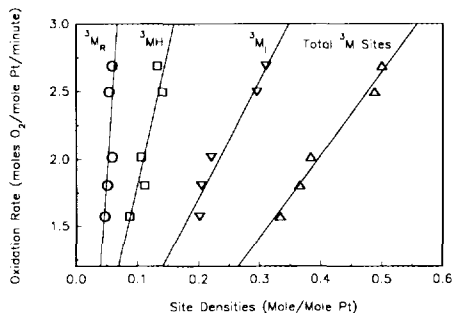


FIG. 1. The relationship between the  $^3M$  site densities and the rates of oxidation of 2-propanol over a series of STO characterized Pt/CPG catalysts.

the nature of the active site promoting a specific reaction all that is needed is to run that reaction over a series of STO-characterized catalysts and to look for a relationship between changes in reaction rate and/or selectivity with changes in the densities of the various types of sites.

The STO characterization data and hydrogen chemisorption results for the 3.35% Pt/CPG (Controlled Pore Glass) catalysts used here are listed in Table 1. Four of these catalysts were prepared by the isothermal reduction of the supported salt precursor in flowing hydrogen at 200, 250, 300, and 400°C and the other was reduced in hydrogen with the temperature ramped between 50 and 400°C at 40°/min.

Each of these catalysts were used for the oxidation of 1.6 *M* solutions of 2-propanol in water at 20°C under one atmosphere of oxygen. All reactions were run at least in duplicate and tested for possible mass transport limitation by using a smaller amount of catalyst, usually one-half, in at least one duplicate run. In all cases the rates normalized to moles of  $O_2$  uptake/mole of Pt were within  $\pm 5\%$  for each catalyst showing that the reactions were not mass transport limited but, instead, were being run in the kinetic regime.

Plots of the initial rates of oxygen consumption (about 20% conversion) against the various STO site densities for the different catalysts as well as the catalyst disper-

sions are found in Figs. 1 and 2. These data show that the only linear relationship is found with the different saturation site,  $^3M$ , densities. The best relationship is between the rates and the total  $^3M$  site densities ( $^3M_1 + ^3M_R + ^3MH$ ). This line has a correlation coefficient of 0.99. No relationship is seen with the  $^2M$  site densities or the  $^1M$  site densities. Comparison of the reaction rates with the catalyst dispersions does give a somewhat linear relationship, but the correlation coefficient for this line is only 0.77.

These results establish that this reaction is taking place on the corner or adatoms on the platinum surface and indicate that the smaller metal particles which have a higher concentration of such atoms on their surfaces should be the more active oxidation catalysts. This is the reverse of the previous observation that the lower dispersed catalysts were more active (11). Since this later observation was made from reactions run under higher oxygen pressures than used here, it could have been the result of a more facile oxidative deactivation of the smaller particles in the catalysts. These data also come from a study in which many of the reactions were run under mass transport limiting conditions (11).

#### Specific Site Rate Factors

Since there are three different types of sites which promote this oxidation, the overall reaction rate must be the sum of the rates of reactions taking place at each of these sites as described in Eq. (1) (41, 46). (Note: all equations are listed in the Appendix.) Here Rate is the observed turnover frequency (TOF) in moles of  $O_2$  uptake/mole of Pt/min, the terms in [ ] are the STO site densities in moles site/mole Pt and the *A*, *B* and *C* are the site TOFs in moles of  $O_2$  uptake/mole of site/min. Using the observed TOF data listed in Table 2 and the STO site data from Table 1 for each catalyst and solving the simultaneous equations a value of 5.5 moles of  $O_2$ /mole of  $^3M_1$  site/min is obtained for *A*, 7.9 moles of  $O_2$ /mole of  $^3M_R$  site/min for *B* and 5.0 moles of  $O_2$ /

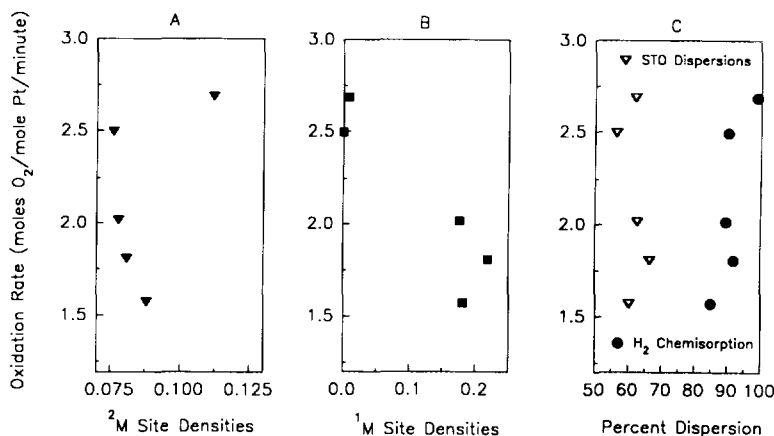


FIG. 2. The relationship between the oxidation rate of 2-propanol using a series of STO characterized Pt/CPG catalysts and their: (A)  $^2M$  site densities, (B)  $^1M$  site densities, and (C) STO and H<sub>2</sub> chemisorption dispersion values.

mole of  $^3MH$  site/min for C. Putting these values and the STO site densities back into Eq. (1) calculated rates can be obtained. These are also listed in Table 2 and show a good correlation with the observed values.

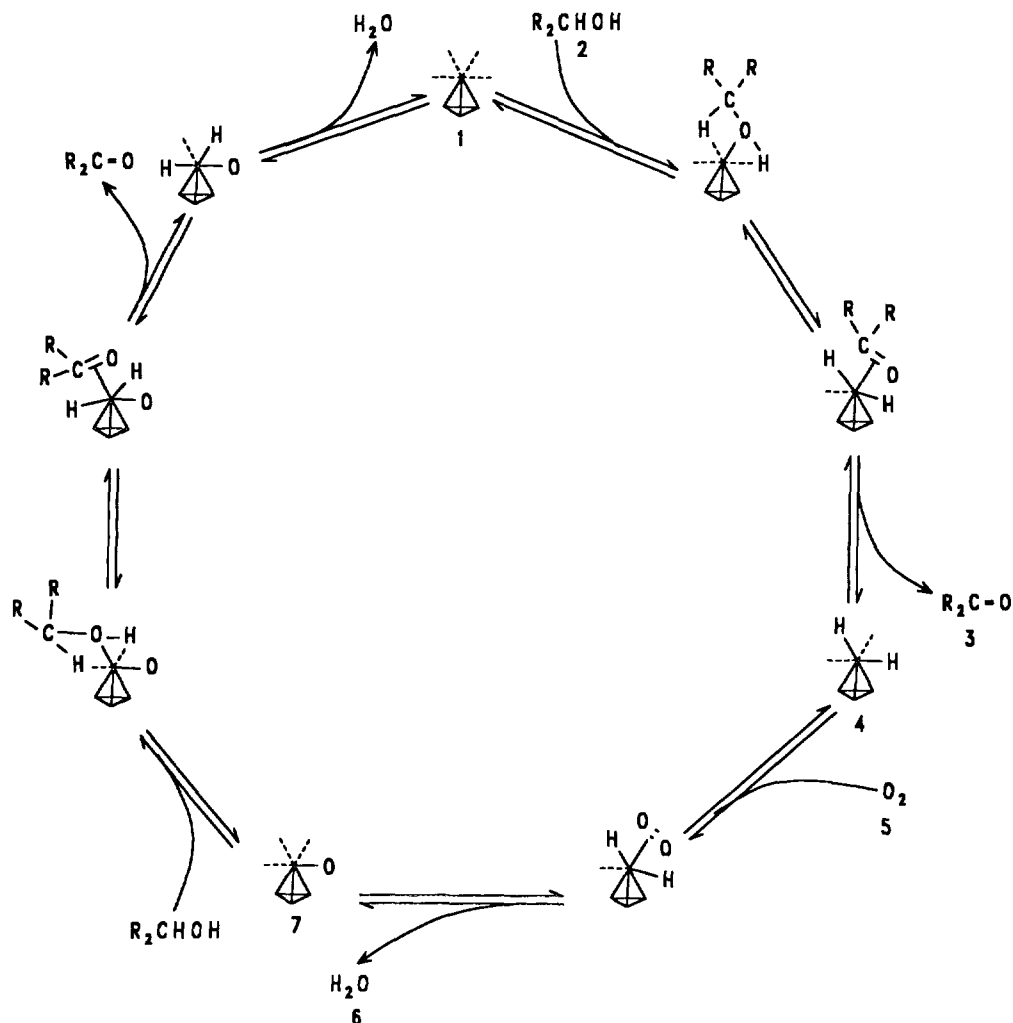
The specific site TOFs for each of the three catalytically active sites are almost the same showing that the oxidation of 2-propanol proceeds with almost equal facility on each of the STO saturation sites. As mentioned previously, published data support a mechanism for this reaction which proceeds through the initial dehydration of the alcohol followed by the reaction of the adsorbed hydrogen with oxygen (11, 28–33). The reaction is taking place on the coordinately unsaturated  $^3M$  sites as proposed in Scheme 1. Each of the different types of  $^3M$  sites, which are corners or analogous atoms, are sufficiently unsaturated to adsorb all of the reactants in this sequence. Beyond that, there is no special step in which one of these sites would be expected to be more or less active than the others.

#### Kinetic Evaluation

While these data show which sites are active and what their activities are, it does not provide information that can be used to calculate equilibrium values for the adsorp-

tion of 2-propanol and oxygen on the catalyst or to determine the rate constant for the rate determining step of the reaction. To obtain these parameters a detailed kinetic analysis of the proceeds is needed. Commonly, this would involve the development of a kinetic expression for the proposed mechanism and then a comparison of this with experimental results. With a proposed mechanism as complex as that proposed in Scheme 1, this is not a straightforward task. With the various degrees of substrate adsorption and different possible rate determining steps a number of kinetic expressions would have to be developed. It is possible that some of these may have the same mathematical form but the constants would have different elementary meanings depending on the assumptions made so correlation with experimental results would be extremely difficult (47). There is, however, an alternate approach.

The development of classical Langmuir-Hinshelwood kinetics is based on the simple reaction shown in Eq. (2) with the adsorption coefficient,  $K_a$ , given by Eq. (4). If the total number of surface sites is given by  $[M_0]$  then, with a unit catalyst surface,  $[M_0]$  becomes one and if  $[S-M]$  is replaced by  $\Theta$ , Eq. (7) becomes the classic Langmuir



SCHEME 1

Isotherm, Eq. (8), with the rate of the forward reaction given by Eq. (9).

If the desorption coefficient,  $K_d$ , described in Eq. (10), is used instead of the adsorption coefficient,  $K_a$ , the reaction rate can be described by Eq. (12). This is the Michaelis-Menten equation (48), the basic equation used for the kinetic investigations of enzyme reactions. Reactions of this type follow saturation kinetics with the rate of reaction changing with variations in substrate concentration as shown in Fig. 3.

Here  $V_{\max}$  is the maximum rate at which

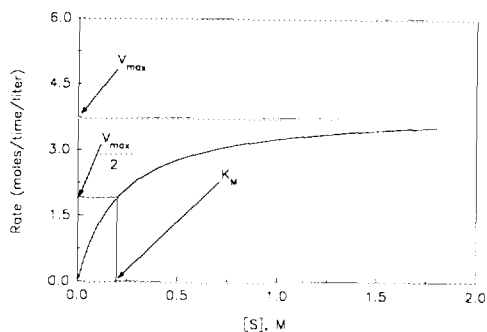


FIG. 3. Relationship between the reaction rate and the substrate concentration.

the reaction can take place when running under zero order reaction conditions with no diffusion constraints. It represents the maximum number of substrate molecules which can be converted to product per active site per unit time; it is the maximum TOF for the reaction. Under these conditions it is related to  $k_{\text{cat}}$  by Eq. (13).  $K_M$  is known as the Michaelis Constant. In simple systems it is equal to  $K_d$ , the true dissociation constant of the  $M-S$  complex. For most purposes, though,  $K_M$  must be considered as an apparent dissociation constant that may be treated as the overall dissociation constant of all adsorbed species.  $K_M$  is the substrate concentration when  $v = 1/2 V_{\text{max}}$ . When there is only one  $M-S$  complex and all adsorption steps are fast,  $k_{\text{cat}}$  is the first order rate constant for the conversion of  $M-S$  into product. More commonly  $k_{\text{cat}}$  is a first order rate constant which is associated with the reactions of all  $M-S$  complexes in the system.

At low values of  $[S]$  the concentration of  $S$  is much smaller than  $K_M$  and the rate of reaction is first order in  $S$  following Eq. (14). When the concentration of  $S$  is large with respect to  $K_M$  the reaction becomes zero order in  $S$  and the rate expression is given by Eq. (15).

The curve in Fig. 3 is a rectangular hyperbola with asymptotes at  $S = -K_M$  and  $v = V_{\text{max}}$ . Since it is difficult to draw such curves accurately and even more difficult to estimate their asymptotes, various forms of graphical representations of the reaction data have been used to obtain values for  $V_{\text{max}}$ ,  $K_M$  and other kinetic parameters of enzyme reactions and others which follow saturation kinetics.

The use of a kinetic approach based on an enzyme kinetic model rather than Langmuir-Hinshelwood concepts is preferred for the reaction depicted in Scheme 1. In the first place this reaction is quite complex so the graphical approach commonly used to determine the mechanism of an enzyme reaction is more practical. Secondly, the basic assumptions of the Langmuir-Hinshelwood

model namely the uniformity of the catalyst surface with each surface atom adsorbing one and only one substrate molecule are not valid. Enzyme reactions, on the other hand, take place by the adsorption and reaction of all substrates on single atom active sites as is the case with the mechanism shown in Scheme 1.

The two-step adsorption reaction sequence proposed for the oxidation of an alcohol (Scheme 1) is analogous to what is called a Ping-Pong mechanism for enzyme reactions. This can be illustrated by Eqs. (16) and (17). In this sequence the metal site,  $M$ , adsorbs a substituent,  $A$ , to give the  $M-A$  complex. This is changed to another complex,  $M'-P$ , which dissociates to give one of the products,  $P$ , and a modified site,  $M'$ .  $M'$  then reacts with the second substrate,  $B$ , to give  $M'-B$  which converts to  $M-Q$  then desorbing the second product,  $Q$ , and regenerating the initial active site,  $M$ .

In the alcohol oxidation reaction (Scheme 1), the catalyst site, 1, is analogous to  $M$ , the alcohol, 2, to  $A$ , the product  $P$  is the ketone, 3, and  $M'$  is the site, 4, on which the hydrogen is adsorbed.  $B$  is oxygen, 5, which adsorbs and reacts with the hydrogen to give water, 6,  $Q$ . In the classic case this would regenerate the active site. In the present reaction, however, a modified active site, 7, which still has one adsorbed oxygen atom, then interacts with a second alcohol molecule. The reaction sequence then progresses through a second dehydrogenation and ketone desorption. This is followed by a reaction between the adsorbed hydrogen and adsorbed oxygen atom to give water and the regeneration of the original active site, 1.

Typically, the kinetics of a bisubstrate reaction such as this are studied by measuring the reaction rates over a range of concentrations of one substrate,  $A$ , while holding the concentration of the second substrate,  $B$ , constant and doing this for several fixed values of  $[B]$  (48). Appropriate graphical analysis of these data, then, distinguishes between the different types of mechanistic



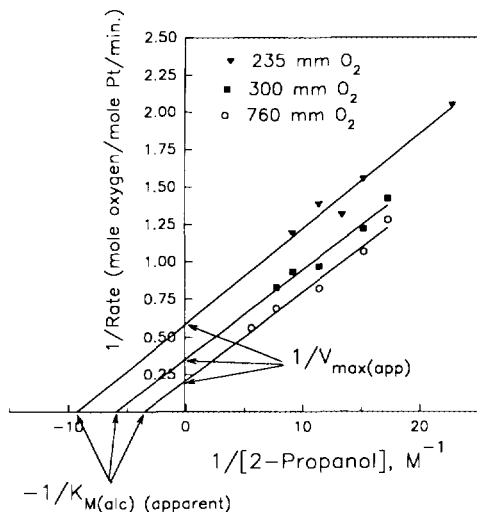


FIG. 4. Lineweaver-Burk double reciprocal plot of 2-propanol oxidations run under various partial pressures of  $O_2$ .

pathways and provides numerical values for the kinetic parameters. One approach to the graphical presentation of enzyme kinetic data is based on the double reciprocal or Lineweaver-Burk plot (48).

The double reciprocal rate expression for this reaction is given by Eq. (18), where  $K_{M(Alc)}$  and  $K_{M(O_2)}$  are, respectively, the dissociation constants for the alcohol and oxygen adsorbed on the catalyst.

The rates of 2-propanol oxidation were measured for reactions run over an 8% Pt/SiO<sub>2</sub> catalyst in water at 20°C. The initial rates of oxygen uptake (about 10% conversion) were determined at three fixed partial pressures of oxygen over a range of alcohol concentrations. The resulting data are listed in Table 3. The partial pressures of oxygen were used to calculate the molarity of the dissolved oxygen at 20°C in water (49). At one atmosphere this was 1.34 mM, at 300 Torr it was 0.53 mM and at 235 Torr it was 0.41 mM. The rates are expressed in moles of oxygen consumed/mole of Pt/min.

The plots of  $1/v$  versus  $1/[Alc]$  for the three partial pressures of oxygen are shown in Fig. 4. The three parallel lines are indica-

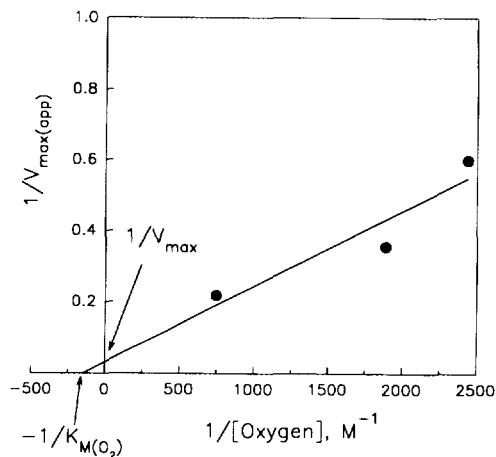


FIG. 5. The replot of the y-axis intercepts of the Lineweaver-Burk graph of 2-propanol oxidation at three partial pressures of  $O_2$ .

tive of a Ping-Pong mechanism and this supports the mechanistic proposal shown in Scheme 1. These lines have slopes of  $K_{M(Alc)}/V_{max}$ , y-axis intercepts of  $1/V_{max(app)}$  and x-axis intercepts of  $-1/K_{M(Alc)(app)}$ . Equations (19) and (20) give the linear forms for these factors.

The replot of  $1/V_{max(app)}$  versus  $1/[O_2]$  is shown in Fig. 5 and that for  $1/K_{M(Alc)(app)}$  versus  $1/[O_2]$  in Fig. 6. In Fig. 5 the y-axis

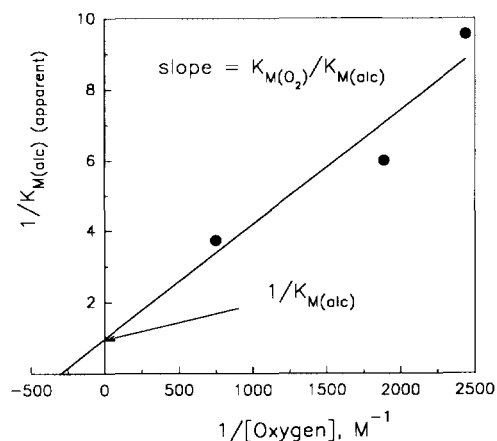


FIG. 6. The replot of the x-axis intercepts of the Lineweaver-Burk graph of 2-propanol oxidation at three partial pressures of  $O_2$ .

intercept gives a value of  $27 \text{ min}^{-1}$  (mole site) $^{-1}$  for  $V_{\max}$  while the  $x$ -axis intercept shows  $K_{M(\text{O}_2)}$  to be  $0.0057 \text{ M}$ . The  $y$ -axis intercept in Fig. 6 gives a value for  $K_{M(\text{Alc})}$  of  $1.0 \text{ M}$  and from the  $x$ -axis intercept a value of  $0.0043 \text{ M}$  for  $K_{M(\text{O}_2)}$ . One reason for this discrepancy in the value of  $K_{M(\text{O}_2)}$  is that only three partial pressures of oxygen were used so the replots had rather poor correlation coefficients.

Both the  $K_{M(\text{Alc})}$  and  $K_{M(\text{O}_2)}$  were also calculated. The lines in the Lineweaver-Burk plot (Fig. 4) have slopes of  $K_{M(\text{Alc})}/V_{\max}$ . From the average value of the three slopes,  $0.060 \text{ minute-mole/liter}$ ,  $K_{M(\text{Alc})}$  was calculated to be  $1.6 \text{ M}$ . Ideally both derivations of  $K_{M(\text{Alc})}$  should give the same value but the relative experimental error was  $\pm 5\%$  for the original rate data and the lines on the Lineweaver-Burk plot were not exactly parallel, their slopes ranged from  $0.058$  to  $0.063 \text{ minute-mole/liter}$ . Also, with only three oxygen concentrations used for the replots a rather poor correlation coefficient of  $0.94$  was obtained. With these factors, then, this discrepancy in  $K_{M(\text{Alc})}$  values is somewhat understandable. As a first approximation an average value of  $1.3 \text{ M}$  was applied to  $K_{M(\text{Alc})}$ . The slope of the line in Fig. 6 is equal to  $K_{M(\text{O}_2)}/K_{M(\text{Alc})}$ . Using  $1.3 \text{ M}$  for  $K_{M(\text{Alc})}$ ,  $K_{M(\text{O}_2)}$  was found to be  $0.0043 \text{ M}$ . Averaging this value with the  $0.0057$  maintained from Fig. 5 gave a value for  $K_{M(\text{O}_2)}$  of  $0.005 \text{ M}$ .

Equation (18), which describes the rate of a Ping-Pong reaction, can be rearranged to give Eq. (21) which describes a rectangular hyperbola, the characteristic shape of rate curves showing substrate saturation kinetics in the plot of rate vs  $[S]$  (48). When the kinetic parameters for 2-propanol oxidation estimated from the Lineweaver-Burk analysis were substituted into Eq. (21) a theoretical rate curve was generated for the reaction at a fixed oxygen concentration. Figure 7 shows both the theoretical and experimentally determined rate curves for 2-propanol oxidation under one atmosphere of oxygen. The fit between theoretical and experimen-

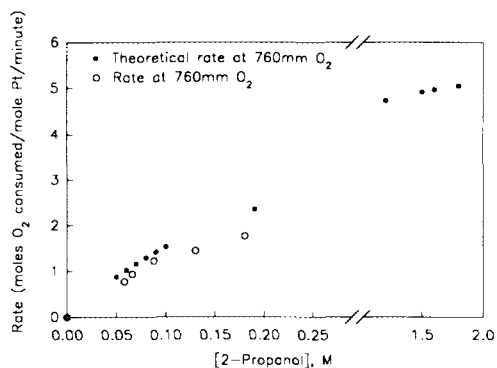


FIG. 7. Comparison of the theoretical and experimental 2-propanol oxidation rates under one atmosphere of  $\text{O}_2$ .

tal is not good so the kinetic parameters were adjusted. To accomplish this an experimental rate curve was fit to Eq. (21) using a curve fitting routine. Keeping the value of  $K_{M(\text{O}_2)}$  as  $0.005 \text{ M}$ , new values for  $K_{M(\text{Alc})}$  and  $V_{\max}$  were calculated using an iterative process. These values were  $18 \text{ min}^{-1}$  for  $V_{\max}$  and  $1.0 \text{ M}$  for  $K_{M(\text{Alc})}$ . With these constants a second theoretical rate curve was calculated and is shown in Fig. 8 along with the experimental curve. An excellent fit is obtained. Since the values for  $K_{M(\text{O}_2)}$  are all relatively close to each other, and the empirically derived  $1.0 \text{ M}$  value for  $K_{M(\text{Alc})}$  was the same as that obtained from Fig. 5 these empirically

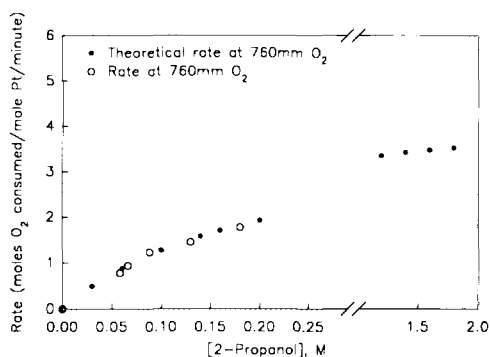


FIG. 8. Theoretical 2-propanol oxidation rates calculated using rate constants obtained from fitting the experimental curve to Eq. (22).

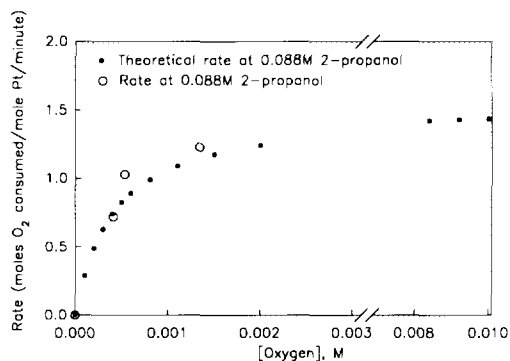


FIG. 9. Comparison of the theoretically determined oxidation rates of a 0.088 *M* aqueous solution of 2-propanol at three partial pressures of O<sub>2</sub> with the experimentally determined values.

derived constants are considered to be reasonably accurate for the present system.

The dissociation constant,  $K_{M(O_2)}$ , for 2-propanol is about two hundred times larger than that of oxygen, 1.0 vs 0.005 *M*, respectively. This indicates that oxygen is bound to platinum two hundred times more strongly than is 2-propanol and that platinum is much more easily saturated with oxygen than with alcohol during these oxidations. This is one reason why the rate data were obtained at only three oxygen concentrations. The rates obtained under one atmosphere of oxygen were already approaching the zero-order region for oxygen concentration dependence as shown in Fig. 9. Thus, the span of oxygen concentrations over which rate data could easily be obtained was limited.

Both the small value of  $K_{M(O_2)}$  relative to  $K_{M(Alc)}$  and the observation that platinum is easily saturated with oxygen support the reported conclusion that oxygen can deactivate the catalyst during alcohol oxidations (11). Complete deactivation of Pt/SiO<sub>2</sub> catalysts was reported after 180 min of reaction and 80–85% alcohol conversion in the oxidation of 2-propanol in water. This deactivation was attributed in part to the oxidation of the platinum. In light of the present data this is not surprising. The oxygen pressures

used were between 1.34 to 3 atm and these pressures correspond to oxygen solubilities of 0.0018 and 0.004 *M*, both of which are either in the zero-order region or close to it from the plot shown in Fig. 9. These reactions were also reported as being zero order in oxygen (11). Given that these experiments were conducted under oxygen saturation conditions and that the  $K_{M(O_2)}$  is two orders of magnitude greater than  $K_{M(Alc)}$ , the problem with oxygen poisoning of the catalyst surface is not surprising.

As indicated above the  $V_{max}$  for this reaction has been found to be about 18 min<sup>-1</sup>. For simple reactions which both adhere to the Michaelis–Menten mechanism and involve only one substrate,  $V_{max}$  is the first-order rate constant for the conversion of the adsorbed complex into the product. In the present case, however,  $V_{max}$  is a function of all first-order rate constants of the forward reaction path and represents the maximum number of molecules converted per active site on the catalyst per unit time if the reaction is zero order in both reactants and has no diffusion limitations. Actually, this value for  $V_{max}$  states that no more than 18 moles of oxygen can be consumed per mole of active site per minute. This corresponds to the 36 moles of acetone produced or 36 moles of C–H bond cleavage. Since there is generally only one active site per enzyme the direct correspondence of  $V_{max}$  to a turnover frequency per active site is straightforward. There are, however, three types of sites which are active in this Pt catalyzed oxidation. As the data in Table I show, the <sup>3</sup>M<sub>I</sub> sites represent about 44% of the active sites present on the Pt/SiO<sub>2</sub> catalyst while the <sup>3</sup>M<sub>R</sub> and <sup>3</sup>M<sub>H</sub> sites each comprise about 28% of the total. These values, combined with the specific site TOF's determined for this reaction give an overall TOF for this catalyst of about 6 min<sup>-1</sup>. Since the reaction conditions needed for zero order oxygen dependence also cause catalyst deactivation (11) and potential diffusion limitations, the present reaction was investigated under first order reaction conditions in both reactants.

Given this discrepancy, the correlation between the observed TOF and  $V_{\max}$  is not unreasonable.

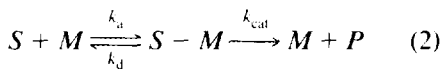
### CONCLUSIONS

The platinum catalyzed oxidation of 2-propanol was run over a series of STO characterized 3.35% Pt/CPG catalysts and the observed rates plotted against the densities of the various types of STO sites. The only linear relationships observed were with the STO saturation sites,  ${}^3M_I$ ,  ${}^3M_R$  and  ${}^3MH$ . From the rate data and site densities of these sites the turnover frequencies for these sites were found to be 5.5, 7.9, and 5.0 moles of oxygen consumed/mole of site/min, respectively.

Initial rate data were obtained for reactions run at several 2-propanol concentration at three separate oxygen pressures. These data were analyzed using the double reciprocal Lineweaver-Burk method commonly employed in enzyme kinetic determinations (48). The data obtained showed that oxygen was adsorbed about 200 times more strongly than 2-propanol in these reactions. A maximum rate value of 18 moles of  $O_2$  consumed/mole of active site/min was calculated. This value represents the maximum rate for the reaction when it is run under zero-order conditions for both reactants without diffusion limitations. The present data were obtained, however, under first-order reaction conditions so the experimentally determined TOF of  $6 \text{ min}^{-1}$  is not unreasonable.

### APPENDIX: EQUATIONS

$$\text{Rate} = A * [{}^3M_I] + B * [{}^3M_R] + C * [{}^3MH] \quad (1)$$



$$k_a[S][M] = k_d[S - M] \quad (3)$$

$$K_a = \frac{k_a}{k_d} = \frac{[S - M]}{[S][M]} \quad (4)$$

$$[M] = [M_0] - [S - M] \quad (5)$$

$$K_a = \frac{[S - M]}{[S][M_0] - [S][S - M]} \quad (6)$$

$$[S - M] = \frac{K_a[M_0][S]}{1 + K_a[S]} \quad (7)$$

$$\Theta = \frac{K_a[S]}{1 + K_a[S]} \quad (8)$$

$$\begin{aligned} \text{Rate} &= k_{\text{cat}}[S - M] = k_{\text{cat}} \Theta \\ &= \frac{k_{\text{cat}}K_a[S]}{1 + K_a[S]} \end{aligned} \quad (9)$$

$$d = \frac{k_d}{k_a} = \frac{[S][M]}{[S - M]} \quad (10)$$

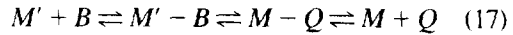
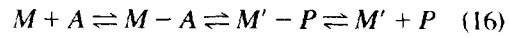
$$[S - M] = \frac{[M_0][S]}{K_d + [S]} \quad (11)$$

$$\text{Rate} = \frac{k_{\text{cat}}[M_0][S]}{K_d + [S]} \quad (12)$$

$$V_{\max} = k_{\text{cat}}[M_0] \quad (13)$$

$$v = \frac{k_{\text{cat}}[M_0][S]}{K_M} = \frac{V_{\max}[S]}{K_M} \quad (14)$$

$$v = k_{\text{cat}}[M_0] = V_{\max} \quad (15)$$



$$\frac{1}{v} = \frac{K_{M(\text{Alc})}}{V_{\max}} \frac{1}{[\text{Alc}]} + \frac{1}{V_{\max}} \left( 1 + \frac{K_{M(\text{O}_2)}}{[\text{O}_2]} \right) \quad (18)$$

$$\begin{aligned} \frac{1}{V_{\max(\text{app})}} &= \frac{(1 + K_{M(\text{O}_2)}/[\text{O}_2])}{V_{\max}} = \frac{K_{M(\text{O}_2)}}{V_{\max}} \frac{1}{[\text{O}_2]} \\ &\quad + \frac{1}{V_{\max}} \end{aligned} \quad (19)$$

$$\begin{aligned} \frac{1}{K_{M(\text{Alc})(\text{app})}} &= \frac{(1 + K_{M(\text{O}_2)}/[\text{O}_2])}{K_{M(\text{Alc})}} = \frac{K_{M(\text{O}_2)}}{K_{M(\text{Alc})}} \frac{1}{[\text{O}_2]} \\ &\quad + \frac{1}{K_{M(\text{Alc})}} \end{aligned} \quad (20)$$

$$\begin{aligned} \text{Rate} &= \frac{v}{[M]} \\ &= \frac{V_{\max} * [\text{Alc}] * [\text{O}_2]}{([\text{Alc}] * [\text{O}_2]) \\ &\quad + (K_{M(\text{O}_2)} * [\text{Alc}]) + (K_{M(\text{Alc})} * [\text{O}_2])} \end{aligned} \quad (21)$$

## ACKNOWLEDGMENT

This research was supported, in part, by Grant DE-FG02-84ER45120 from the U.S. Department of Energy, Office of Basic Energy Science.

## REFERENCES

- Heyns, K., and Paulsen, H., in "Newer Methods of Preparative Organic Chemistry" (W. Foerst, Ed.), Vol. II, p. 303. Academic Press, New York, 1963.
- Sheldon, R. A., *Stud. Surf. Sci. Catal.* **59**, (Het. Catal. Fine Chem.), 33, (1992).
- Heyns, K., and Blazjewicz, L., *Tetrahedron* **9**, 67 (1960).
- Sheeden, R. P. A., and Turner, R. B., *J. Am. Chem. Soc.* **77**, 190 (1955).
- Sneeden, R. P. A., and Turner, R. B., *J. Am. Chem. Soc.* **77**, 13 (1955).
- Fried, J., and Sih, J. C., *Tetrahedron Lett.*, 3899 (1976).
- Heyns, K., and Paulsen, H., *Angew. Chem.* **69**, 600 (1957).
- Heyns, K., and Paulsen, H., *Adv. Carbohydrate Chem.* **17**, 169 (1962).
- Heyns, K., Paulsen, H., Ruediger, G., and Weyer, J., *Fortschr. Chem. Forsch.* **11**, 285 (1969).
- Angyal, S. J., and Anderson, L., *Adv. Carbohydrate Chem.* **14**, 135 (1959).
- Nicoletti, J. W., and Whitesides, G. M., *J. Phys. Chem.* **93**, 759 (1989).
- Van Dam, H. E., Wisse, L. J., and Van Bekkum, H., *Appl. Catal.* **61**, 187 (1990).
- Heyns, K. and Heinemann, R., *Liebigs Ann. Chem.* **558**, 187 (1947).
- Heyns, K. and Stockel, O., *Liebigs Ann. Chem.* **558**, 192 (1947).
- Heyns, K., *Liebigs Ann. Chem.* **558**, 171, 177 (1947).
- Mehrtretter, C. L., Rist, C. E., and Alexander, B. H., U.S. Patent 2,472,168 (1949).
- Dirkx, J. M. H., and van der Baan, H. S., *J. Catal.* **67**, 1 (1981).
- Mehrtretter, C. L., U.S. Patent 2,562,220 (1951).
- Mehrtretter, C. L., Alexander, B. H., Mellies, R. L., and Rist, C. E., *J. Am. Chem. Soc.* **73**, 2424 (1951).
- Heyns, K. and Paulsen, H., *Chem. Ber.* **86**, 835 (1953).
- Barker, S. A., Bourne, E. J., and Stacy, M., *Chem. Ind. (London)*, 970 (1957).
- Aspinall, G. O., Cairncross, J. M., and Nicolson, A., *Proc. Chem. Soc.*, 270 (1959); *J. Chem. Soc.*, 2503, 3998 (1960).
- Saito, H., Ohnaka, S., and Fukuda, S., Eur. Patent 142,725, (1984).
- Smits, P. C. C., Kuster, B. F. M., van der Wiele, K., and van der Baan, H. S., *Carbohydrate Res.* **153**, 227 (1986).
- Smits, P. C. C., Kuster, B. F. M., van der Wiele, K., and van der Baan, H. S., *Appl. Catal.* **33**, 83 (1987).
- Dijkgraaf, P. J. M., Rijk, M. J. M., Meuldijk, J., and van der Wiele, K., *J. Catal.* **112**, 329 (1988).
- Dijkgraaf, P. J. M., Duister, H. A. M., Kuster, B. F. M., and van der Wiele, K., *J. Catal.* **112**, 337 (1988).
- Wieland, H., *Chem. Ber.* **45**, 2606 (1912); **46**, 3327 (1913); **54**, 2353 (1921).
- Alam, M., and Umar, M., *Pak. J. Sci. Ind. Res.* **23**, 140 (1980).
- DiCosimo, R., and Whitesides, G. M., *J. Phys. Chem.* **93**, 768 (1989).
- Rottenberg, M., and Baertschi, P., *Helv. Chim. Acta* **39**, 1973 (1956).
- Sexton, B. A., *Surf. Sci.* **102**, 271 (1981).
- McKee, D. W., *Trans. Faraday Soc.* **64**, 2200 (1968).
- Gillespie, W. D., Herz, R. K., Petersen, E. E., and Somorjai, G. A., *J. Catal.* **70**, 147 (1981).
- Augustine, R. L., and Thompson, M. M., *J. Org. Chem.* **52**, 1911 (1987).
- Augustine, R. L., and Warner, R. W., *J. Org. Chem.* **46**, 2614 (1981).
- Augustine, R. L., Kelly, K. P. and Y.-M. Lay, *Appl. Catal.* **19**, 87 (1985).
- Augustine, R. L., and Warner, R. W., *J. Catal.* **80**, 358 (1983).
- Augustine, R. L., Ewing, G. W., and Ashworth, H. A., *Chem. Ind. (Dekker)* **5**, (Catal. Org. React.), 149 (1981).
- Augustine, R. L., Tanielyan, S., and Wolosh, G., *Chem. Ind. (Dekker)* (Catal. Org. React.), in press.
- Augustine, R. L., Baum, D. R., High, K. G., Szivos, L. S., and O'Leary, S. T., *J. Catal.* **127**, 657 (1991).
- Ledoux, M. J., *Nouv. J. Chim.* **2**, 9 (1978).
- Ledoux, M. J., Gault, F. G., Bouchy, A., and Roussy, G., *J. Chem. Soc. Faraday Trans. 2* **74**, 652 (1978).
- Ledoux, M. J., and Gault, F. G., *J. Catal.* **60**, 15 (1979).
- Ledoux, M. J., *J. Catal.* **70**, 375 (1981).
- Augustine, R. L., Thompson, M. M., and Doran, M. A., *J. Chem. Soc. Chem. Commun.* 1173 (1987).
- Satterfield, C. N., "Heterogeneous Catalysis in Practice," p. 42. McGraw-Hill, New York, 1980.
- Fersht, A., "Enzyme Structure and Mechanism," p. 84. Freeman, San Francisco, 1977.
- Lange, N. A., "Lange's Handbook of Chemistry," p. 1264. Handbook Publishers, Sandusky, OH, 1949.